

Investigating the Fracture Toughness and Mechanical Properties of the Two-Layer Al 1050/Mg AZ31B Sheets Fabricated by the Roll Bonding, Considering the Annealing Temperature Effect

Payam Tayebi, Ramin Hashemi*

* rhashemi@iust.ac.ir

School of Mechanical Engineering, Iran University of Science and Technology, Tehran, Iran

Received: September 2024

Revised: December 2024

Accepted: March 2025

DOI: 10.22068/ijmse.3749

Abstract: This study presents the manufacturing of Al 1050/Mg AZ31B bimetallic sheets using the roll bonding process, followed by an investigation of the effect of annealing temperature on mechanical properties and microstructural features. Annealing treatment was performed at 200, 300, and 400 degrees Celsius. Mechanical testing includes tension, micro-hardness, three-point bending, and fracture toughness. Scanning electron microscopy equipped with energy-dispersive X-ray spectroscopy (SEM-EDX) and X-ray diffraction (XRD) were used to investigate the microstructure in the infiltration zone. Mechanical testing shows that increasing the annealing temperature decreases the tensile strength of the two-layer specimens. Micro-hardness, XRD, and SEM-EDX investigations confirm the presence of intermetallic particles in the penetration zone. The micro-hardness test showed that with the increase of the annealing temperature, the hardness in the penetration zone of Al 1050/Mg AZ31B increases. The results show an increase of 185% compared to the Mg base sheet and 200% to the Al base sheet. This increase in micro-hardness result confirms the presence of harder intermetallic phases with increasing annealing temperature in the penetration zone. Also, fracture toughness test results show an increase of 160 percent compared to the Al base sheet and 225 percent compared to the Mg base sheet.

Keywords: Fracture toughness, Mechanical properties, Al 1050/Mg AZ31B sheets, Roll bonding process, Annealing.

1. INTRODUCTION

Metals with a low strength-to-weight ratio are widely used in aerospace, automobile, and electronics industries. The lightest structural material is Mg, which has desirable properties for transportation applications. However, Mg alloys are limited compared to Al ones due to their poor formability and corrosion resistance. One approach to increase the formability of Mg sheet alloys is by increasing their forming temperature, which activates hard slip modes and results in dynamic recrystallization. Studies have shown that using an Al layer on the surface of Mg as an Al-Mg two-layer can improve the corrosion resistance of Mg alloys [1, 2]. Various methods, such as accumulative roll bonding (ARB) [3], explosive welding [4], and rolling processes, have been used to produce Al/Mg multilayer sheets. Nie et al. [5] investigated microstructure properties for Al/Mg/Al composite fabricated by ARB process up to four cycles. Strength increases in the third cycle, and after the third pass, they decrease again.

Cheepu et al. [6] Investigated the effect of preheating temperature parameters on mechanical and metallurgical properties of 3-layer Al and Mg

sheets. They found that the bond strength of the layers depended on the annealing temperature, time, and number of rolling passes. Habila et al. [3] Investigated the mechanical and microstructural behaviors of a 3-layer Al/Mg/Al sheet fabricated by ARB up to 5 cycles. They found that the mechanical properties increased up to 3 cycles, but from 3 to 5 cycles, decreased in strength. Yang et al. [7] reported that the intermetallic between Al and Mg layers were Al_3Mg_2 and $Al_{12}Mg_{17}$. Rouzbeh et al. [8] produced a two-layer sheet by explosive welding and rolling. They found that the penetration depth in the rolling process is more significant than in the explosive welding process. Nie et al [5]. The 3-layer Al/Mg/Al sheet by ARB process in 4 states was preheated at 400°C for 5 minutes. They showed that Al/Mg multilayer samples have good formability under preheated conditions. Nie et al [9]. produced the Al/Mg/Al sheet by the hot rolling process at 400 degrees. The samples were then annealed at temperatures between 200 and 400°C for 1 to 4 hours. They then investigated the mechanical properties and failure surface for different annealing conditions. Macwan et al [10]. studied the annealing temperature effect on the interface intermetallic compounds of the Al/Mg

layer and intermetallic phases. They found that enhanced annealing temperature increases the intermetallic layer's thickness. Jalali et al [11]. investigated the mechanical properties of the two-layer Al/Br sheet and found that the strength of the two-layer sheet is between the base sheet of Br and Al.

Nie et al. [12] investigated the effect of the annealing process on the formability of the Al/Mg/Al sheet by the deep drawing method. They showed that increasing the annealing temperature will increase the ductility. Rahmatabadi et al. [13] used Nakajima and Erickson's test to study the FLD of Al/Mg bimetal. They showed that the ultrasonic vibration FLD diagram has a higher strain than standard forming methods. Delshad et al. [14] studied the influence of the annealing process on the formability of the 3-layer sheet. They found that strength and hardness will decrease with increasing annealing temperature. Rahmatabadi et al. [15] produced an Al and Mg alloy composite using the ARB process. They studied the mechanical and microstructural properties of the composite at different rolling cycles. Han et al. [16] studied the result of annealing temperature and time on the intermetallic compound. They found that the intermetallic compound increases in the two-layer sheet with increased annealing time and temperature.

As shown in the above studies, most of the studies conducted in the past have examined the effect of annealing temperature on intermetallic phases. However, in this study, in addition to investigating the effect of annealing temperature on the strength of the infiltration layer and intermetallic phases, mechanical effects, including fracture toughness and three-point bending test, were also investigated. Also, quantitative studies related to XRD by MAUD software for a two-layer Al 1050/Mg AZ31B sheet were carried out for the first time. This study investigated the effect of annealing temperature on dislocation density and grain size.

2. EXPERIMENTAL PROCEDURES

2.1. Material

In this study, the sheet plates used are AZ31B (thickness= 1 mm) and Al 1050 (thickness= 2 mm), respectively, in their as-received condition. The base sheets' chemical compositions are

shown in Table 1. The craniometric test was used to analyze the chemical composition of the Al and Mg samples. Samples were cut to 135 mm and 75 mm in length and width, respectively.

2.2. Roll Bonding Process

Before the roll bonding, samples were cleaned with acetone to remove grease. Next, a wire brush was used to remove the oxide layer. Then, the samples were fastened in 2 layers on each other. Next, the fixed plates were heated for 10 min at 400°C in a furnace before the roll bonding process. The Roller diameter was 40 cm, and the speed was 6 rpm.

2.3. Annealing Process and Metallurgical Study

An annealing treatment was carried out to eliminate the effect of residual stresses caused by the rolling process and work hardening; temperature and holding time significantly influence the diffusion rate at the Mg/Al interface [17]. The intermetallic phase will not be formed for the two-layer sheet if the infiltration layer's annealing temperature is below 200°C. If the annealing temperature exceeds 400°C, the infiltration layer can melt at the interface [18].

To determine the appropriate annealing temperature, samples were subjected to various annealing temperatures, 200°C, 300°C, and 400°C, for 1.5 hours. Then, after the annealing process, the mechanical properties of two-layer samples were determined in 4 samples: 1- ambient temperature, 2- 200°C, 3- 300°C, and 4- 400°C. Also, Field emission scanning electron microscopy (FESEM) and Energy Dispersive Spectroscopy (EDS)-LINE-Map were utilized to investigate the effect of annealing temperature on the penetration depth and fracture type of the two-layer samples. The cross-sectional sample prepared from the 2-layer samples for SEM was first prepared by cold mounting, and then the samples were prepared for imaging by sanding up to 3000 grit and final polishing.

Considering the possibility of forming intermetallic phases at high temperatures for Al and Mg alloys, investigations were carried out by X-ray powder diffraction (XRD) with grazing method and 20° to 80°. For the X-ray test, the cross-sectional area of the 2-layer samples was examined.

Table 1. The chemical composition for base sheets (wt.%)

	Al	Sb	Ni	Mg	Zn	Fe	Cu	Si	Mn
Al1050	99/8	0/02	0/003	0/005	0/196	0/472	0/095	0/096	0
Mg Az31B	2.45	0	0	97/36	0/294	0/004	0	0/049	0/186

2.4. Mechanical Testing

To investigate the effect of rolling and cold working on the mechanical properties of two-layer composites, they were evaluated using tensile testing, hardness measurement, and 3-point bending test for specimens annealed at various temperatures and fracture toughness at ambient temperature.

2.4.1. Tensile test

To compare the mechanical properties in different annealing temperatures, tensile tests according to the ASTM-E8M standard were done [19]. A sub-size sample was used to prepare the tensile test sample. Fig 1 shows the dimension of sample size and examples of the prepared tensile test specimens. A 5-ton tensile device did the tensile test, and with 2 mm/min speed test

was done.

2.4.2. Vickers hardness and three-point bending test

To characterize the interface of the AA1050/Mg-AZ31B two-layer (Fig. 2), Vickers micro-hardness was performed across the specimen thickness. Micro-hardness testing was performed for two-layer samples in different annealing temperatures. The indentation load applied to the specimens was 100 gr for 15 s.

A three-point bending test was performed to determine the bending properties of two-layer samples. Testing was done at room temperature using a tensile tester with a 0.5 mm/min displacement rate. The three-point bending test samples were 10 and 100 mm wide and length, respectively.



Fig. 1. a) Tensile test specimen design according to ASTM-E8M, b) prepared tensile test sample

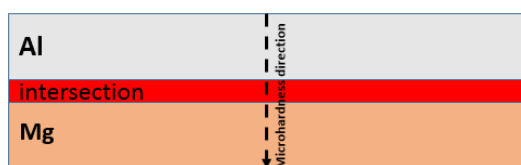


Fig. 2. Micro-hardness direction

2.4.3. Fracture toughness

The fracture tests were performed to evaluate

stiffness characterizations of as-rolled two-layer composite and base metal at room temperature. To do this, compact tension (CT) samples were prepared according to ASTM-E 647 [20]. The sample size is shown in Fig. 3. To check the crack growth in the sample, a camera with one frame per second imaging was used (Fig. 4). The test rate was 0.5 mm/min. The crack growth rate was obtained using Image-j software.

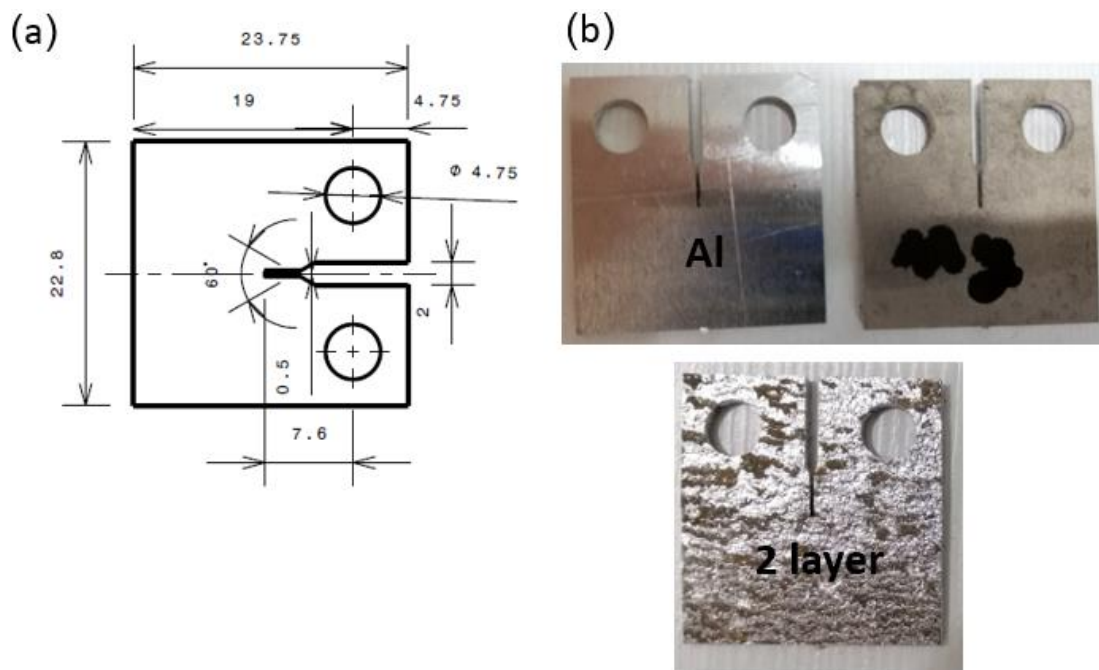


Fig. 3. a) Sample size, b) fracture toughness sample

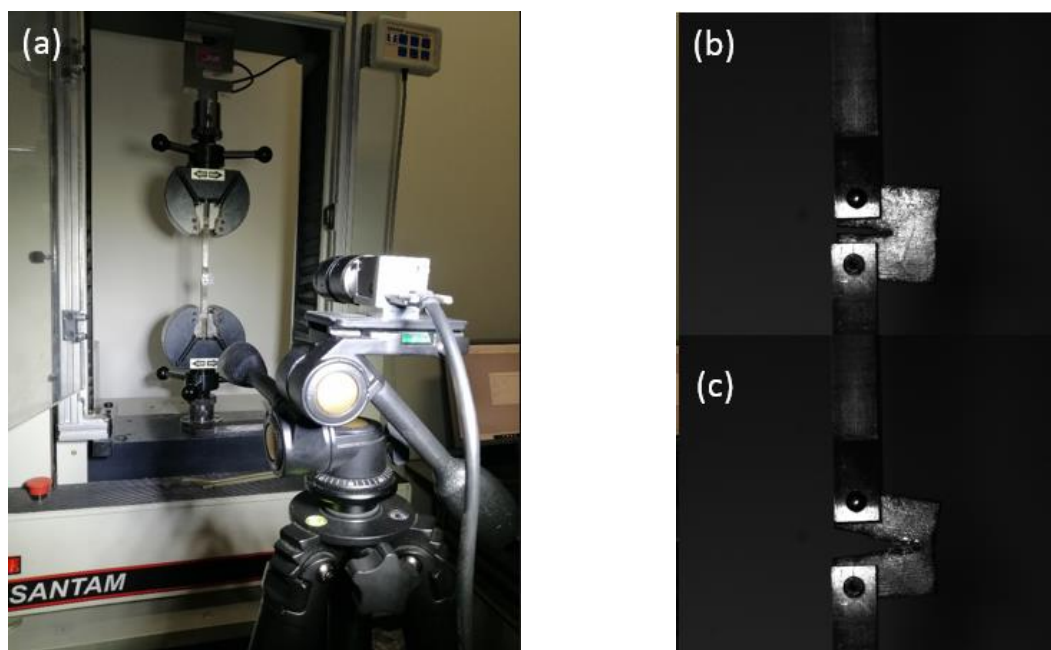


Fig. 4. a).Setup of the fracture toughness, b) before start test, C) end test

3. RESULTS AND DISCUSSION

In this article, two-layer Al/Mg sheets were produced using the rolling bond process. Next, relevant mechanical and metallurgical tests were carried out to investigate the effects of work hardening and annealing temperature on the mechanical and metallurgical properties. During the annealing process, after the rolling process, three different occurrences will occur, and the effect of each of these occurrences on the strength of the layer bond will be studied [21]:

- The annealing operation will reduce the hardness of the sheet, and as a result, the toughness of the bond will increase. In this case, the force required for crack growth increases, and bond strength increases.
- The annealing process causes the residual stress in the penetrating layer to decrease or disappear, in which case the bonding strength will increase.
- The phenomenon of the brittle intermetallic phase formation in the penetration zone will decrease the bonding strength

The interlayer strength will decrease if the percentage of brittle intermetallic phases in the microstructure increases with increasing annealing temperature. In summary, increasing the annealing temperature will increase the layer bond strength to some extent, and from a higher temperature (the temperature at which brittle intermetallic phases are formed), it will decrease the bond strength.

Considering the above, the following sections present an analysis of the effect of annealing temperature on metallurgical and mechanical properties.

3.1. Penetration Depth Study

Microstructural investigations were carried out for two-layer samples to investigate the effect of annealing temperature. SEM and ESD-Line scans were performed to measure the diffusion of Al and Mg alloys into each other. In Fig. 5, the composition percentage of Al and Mg elements in the EDX map was measured in addition to the penetration depth. The penetration speed of two atoms in a two-component solution is not the same, and the element with a lower melting point penetrates faster [22]. In general, atoms move in the crystal lattice due to the movement of vacancies.

The diffusion coefficient is a function of chemical composition and temperature. Diffusion in metals In addition to intercrystalline diffusion, diffusion occurs along grain boundaries between crystals. The diffusion rate along the grain boundary will happen faster than within the crystal. One of the things that prevents penetration into metals is impurities. If the temperature increases, dislocations will be eliminated. Their density at the grain boundaries will decrease due to the increase in grain size, and as a result, the penetration at the grain boundary will increase. By examining the ESD-Line results, it was found that the penetration depth increases with the increase in annealing temperature [23]. This increase in penetration depth can be considered due to an increased penetration rate at high temperatures [20, 21]. One of the reasons for the increase in penetration depth at higher temperatures is the surface tension of grain boundaries and the dynamics of grain boundaries at high temperatures [24]. It can be seen (Fig. 5) that with the increase of temperature in the two-layer samples, the slope of the graph for Mg metal relative to Al metal decreases, which indicates the infiltration of Mg in Al.

3.2. Intermetallic Phase Analysis

As shown in Fig. 6, the EXPERT High Score Plus software result analysis, XRD patterns of intermetallic phases were detected, and the effect of annealing temperature on the intermetallic phase formation for the two-layer sample. By examining the researchers' studies, it was found that at different annealing temperatures, it is possible to make an intermetallic phase in the infiltration layer of Al and Mg [13, 17]. According to the XRD results, it can be seen that three intermetallic phases $Al_{0.58}Mg_{0.42}$ [26], $Al_{12}Mg_{17}$ [13, 25, 26], and Al-Mg are formed in two-layer samples for annealing temperatures of 200°C, 300°C, and 400°C. $Al_{0.58}Mg_{0.42}$ phase forms at a lower temperature than compared to $Al_{12}Mg_{17}$ phase [29]. The XRD results have been validated by comparing the reference results with the pick list title. Studies show that increasing annealing temperature and holding time will form more intermetallic phases [30], detrimental to the mechanical properties. According to [22, 23], intermetallic compounds with a diameter of fewer than 10 μm for the joining area of dissimilar metals do not harm the joint's quality.



Fig. 5. EDS-Line and Map analysis for Al/Mg Samples, a) environment temperature, b) 200°C annealing, c) 300°C annealing, d) 400°C annealing

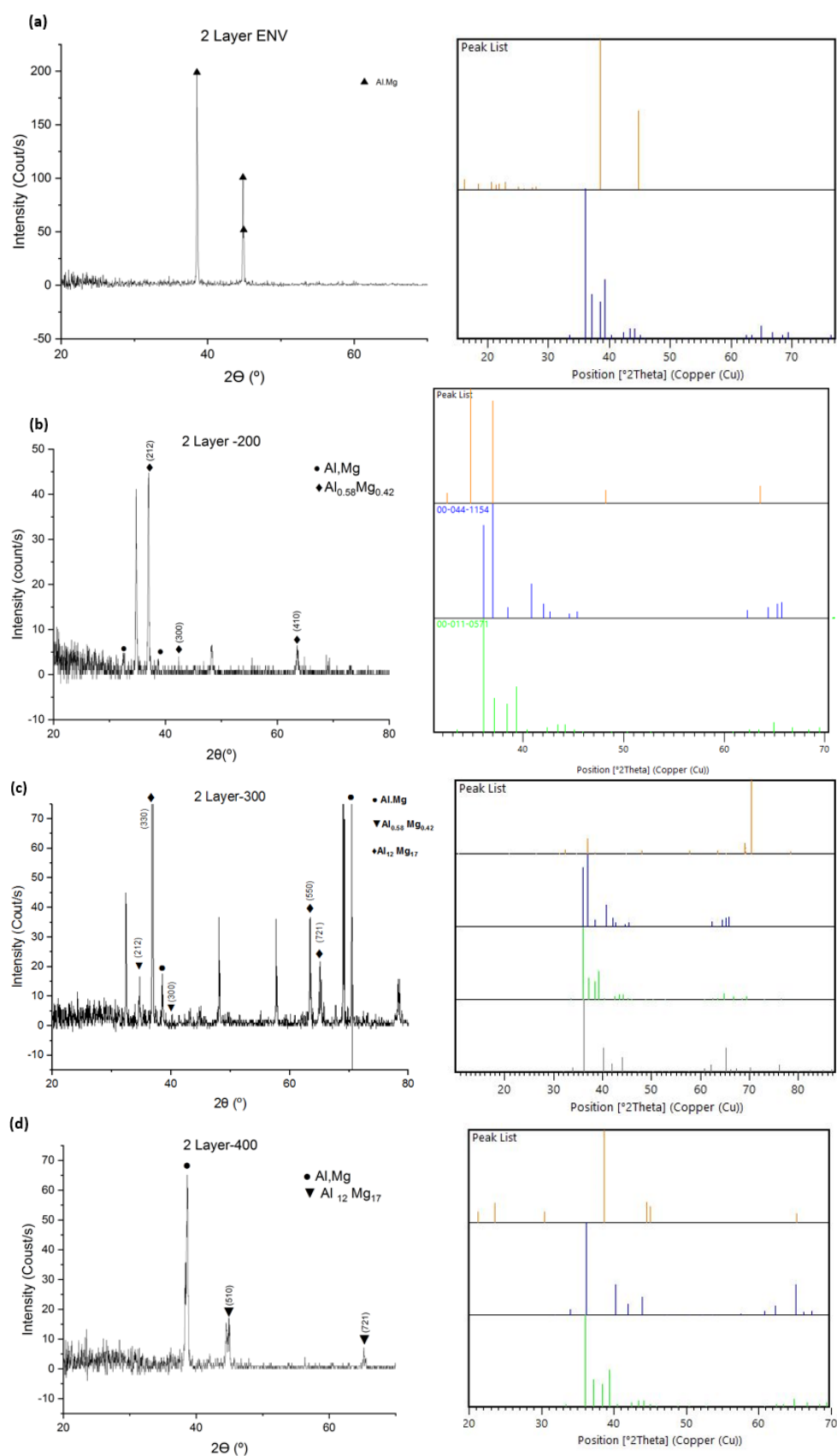


Fig. 6. XRD results and reference results for the two-layer sample, a) environment temperature, b) 200°C annealing, c) 300°C annealing, d) 400°C annealing

Given that the formation of intermetallic phases occurs due to the phenomenon of intermetallic diffusion or the phenomenon of intercalation or substitution of atoms, annealing temperature and time are effective parameters in the formation of the type and size of intermetallic phases (according to the aluminum-magnesium equilibrium diagram). The strength increase due to intermetallic phases depends on the size of the secondary phases and the distribution of the secondary phases in the matrix phase. In the microstructure, intermetallic phases act as a barrier against the movement of dislocations. As a result, the formation of intermetallic phases with a larger diameter can delay the movement of dislocations and increase the strength of the metal. Moreover, it can contribute to precipitation hardening and result in improved strength. In the following, the XRD results were analyzed using the numerical software MAUD using the Rietveld method. Quantitative results obtained from MAUD software for Crystallite Size and internal micro-strains are shown in Fig. 7-a and 7-b, respectively. The results show that the crystallite size will increase with increasing annealing temperature, and the micro-strain will decrease. Considering that in the process of recrystallization, the energy

required for grain growth is obtained from the strain energy stored during deformation, as stated, with increasing annealing temperature, grain growth can be expected in exchange for reducing the internal micro-strain [22]. Theoretically, it can be observed that the dislocation density will decrease with the increase of the annealing temperature and recrystallization process. As a result, ductility will increase, and strength will decrease [33, 34]. In Eq. 1, ϵ is the internal micro-strain, d is the crystallite size, and b is the Burgers vector. Fig. 7-c shows the results for dislocation density. With the increase in the annealing temperature, the dislocation density in the two-layer sample is clearly decreasing. Among the reasons for the decrease in the density of dislocations with the increase in the annealing temperature are the increase in the grain size, the decrease in internal strains, and the decrease in residual stresses.

$$\rho = \frac{2\sqrt{3}\epsilon}{db} \quad (1)$$

3.3. Tensile and Micro-Hardness Test Result

Uniaxial tensile and hardness tests were investigated to study the mechanical properties of the base sheet and the two-layer samples.

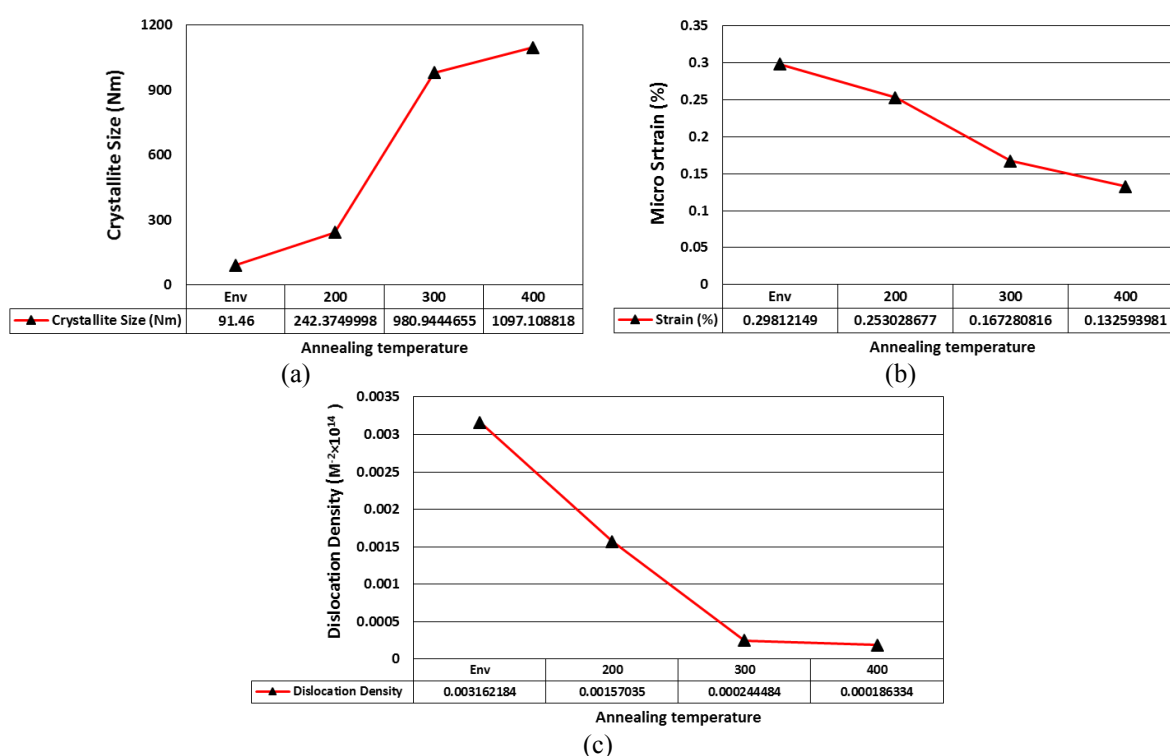


Fig. 7. Effect of annealing temperature on microstructural properties, a) Crystallite Size, b) Micro-Strain, c) Dislocation density

Figures 8 and 9 show the stress-strain curves for base sheets and two-layer samples. The tensile test results show that the tensile strength of the two-layer sample (193.69 MPa) has increased by 120% compared to the Al base sample (88.64 MPa), and it has decreased by 5% compared to the Mg base sample (203.43 MPa). As in Fig 11-b, it was found that increasing the annealing temperature will reduce the strength of the two-layer samples. The most significant reduction of the strength of the Al/Mg composite occurs at a temperature of 400°C. The reasons for this decrease in strength can include the recrystallization and growth of new grains and the decrease of the dislocation density due to the annealing process [35] (according to Fig. 9-c).

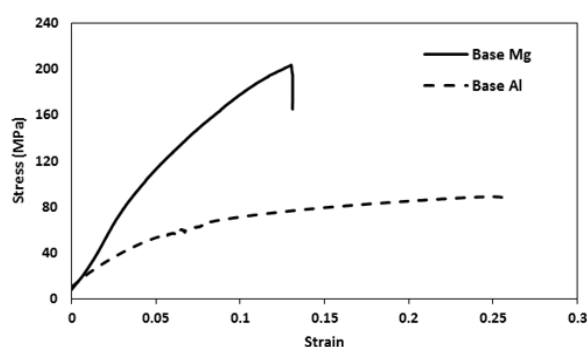


Fig. 8. Engineering Stress-Strain curves of Base sheet

On the other hand, it can be seen that at the 200°C annealing temperature, the strain has increased compared to the ambient temperature. Still, as the annealing temperature increases from 200°C, the strain will decrease. One of the reasons for reducing the strain at higher annealing temperatures is the decrease in the bonding strength area with increasing temperature. The Kirkendall effect can explain the cause of the

strain reduction. In this case, the voids move against the direction of movement of atoms and accumulate in the form of tiny holes, which causes that during the tensile test, these defects act as areas of stress concentration and cause crack propagation and failure [36].

The results of the micro-hardness for the base sheet sample and the two-layer sample are shown in Fig. 10. By examining Fig. 10, it can be seen that the hardness obtained from the two-layer samples due to the hard work performed on the rolled samples increased the hardness values in the Mg and Al areas compared to the base sheets. This increase has correspondingly increased by 185% for the Mg area of the two-layer sample compared to the Mg base sheet and by 200% for the Al area of the two-layer sample compared to the Al base sheet. This increase in hardness occurs due to the increased density of dislocations and cold working [37]. However, the hardness of the penetration zone at room temperature has decreased by about 64% compared to the Mg base sheet and increased by about 240% compared to the Al base sheet.

In Fig. 10-b, in the penetration zone, it is clear that the hardness at the annealing temperature of 400°C suddenly increases to about 187.55 due to the presence of harder intermetallic phases [10], which are mentioned in the XRD results [16]. As mentioned above, increasing the annealing temperature usually will decrease the dislocation density and grain size, decreasing the hardness. However, if increasing the annealing temperature causes the formation of hard intermetallic phases, increasing the annealing temperature cannot decrease the hardness, which happened for the annealing temperature of 400°C in the penetration zone.

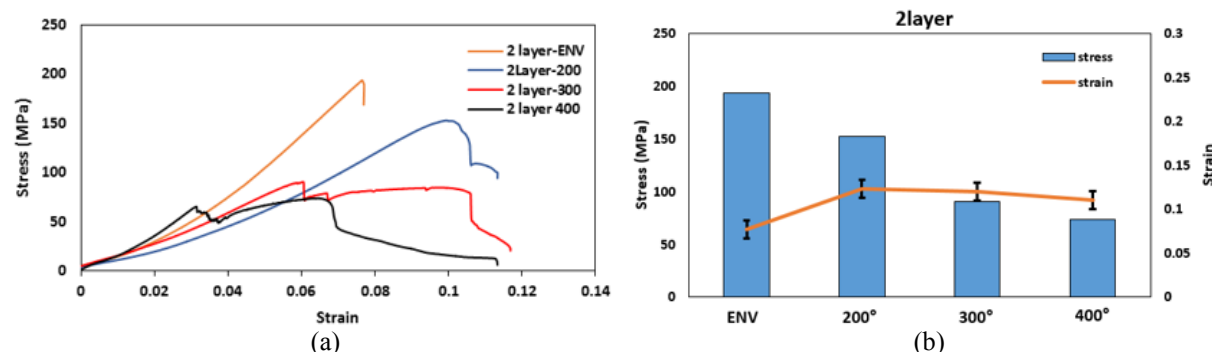


Fig. 9. a) Engineering Stress-Strain curves of two-layer sheets in environment temperatures, 200°C, 300°C and 400°C, b) Investigating the effect of different annealing temperature conditions on strain and stress

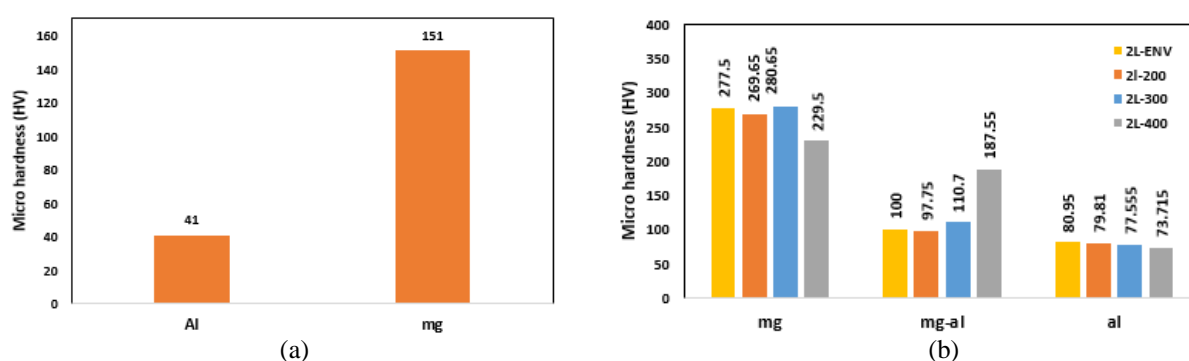


Fig. 10. a) Micro-hardness result for base sheets b) Micro-hardness result for two-layer sheets in environment temperature, 200,300 and 400 degree

Strength and hardness in metals are directly related and inversely related to formability. Several factors can increase the solid-state strength in the microstructure. These factors include strengthening by 1- grain size reduction, 2- solid solution, 3- work hardening, 4- secondary phases, 5- precipitation hardening, and 6- crystal lattice defects. Due to the cold working process performed during the rolling process to produce two-layer samples, the strength of the two-layer samples has increased [38]. The samples were then annealed, allowing intermetallic phases to form in the microstructure. The presence of intermetallic phases in the microstructure will increase the strength.

3.4. Three-Point and Fracture Toughness Analysis

This section checks the properties of fracture toughness and three-point bending for the base and two-layer sheet samples, which were done only for room temperature conditions. Fig. 11 presents load-deflection curves of the Al/mg multilayered composites after the CRB process and Al and Mg base sheets. By examining the graph obtained from the three-point bending test, it is clear that the bending force for the two-layer sample is equal to the force of the base sheets. The three-point bending results show that the strength of the interlayer bond in the two-layer sample is optimal compared to the base metal. Nevertheless, due to cold work and reduced formability in the two-layer sample, the sample failed at a lower depth than the base sheets. This indicates the crispness of the two-layer sample.

To investigate the effect of the rolling process, the fracture toughness test was performed for the two-layer AL/Mg samples and the Al and Mg base sheet samples and considering the plane

stress conditions.

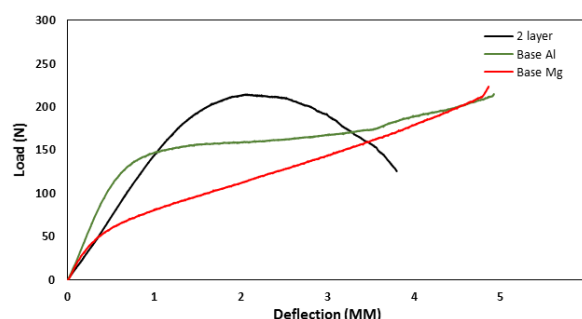


Fig. 11. Force-deflection curves of the Al/Mg multilayered Sheet tested by three-point bending load

According to the sample preparation for the fracture toughness test (Fig. 5), the fracture toughness test was performed, and the test results are in the form of a force-displacement diagram in Fig. 12 has been shown.

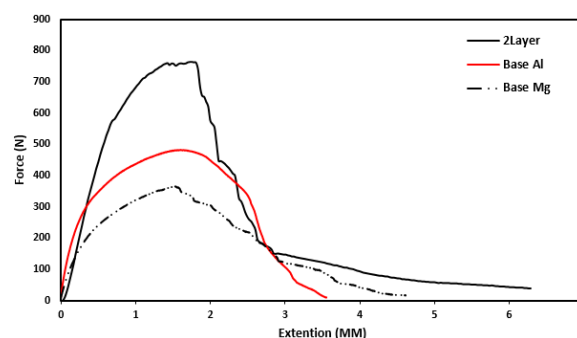


Fig. 12. Force-extension curves of the Al/Mg multilayered Sheet

The critical load of the sample must be determined first to determine the fracture toughness. Critical load refers to the load at which the crack grows [39]. After obtaining the fracture toughness test forces and with the help

of images prepared during the test from the crack growth rate, corresponding to the crack growth rate at different times and the corresponding force, the fracture toughness will be calculated. According to the standard ASTM-E 647 and Eq. 2 and 3, calculations related to fracture toughness were performed.

$$K_Q = \left(\frac{P_Q}{B \times W^{0.5}} \right) \times f\left(\frac{a}{W}\right) \quad (2)$$

The value of the correction factor $F\left(\frac{a}{W}\right)$ is calculated from Eq. 2.

$$f\left(\frac{a}{W}\right) = \left[\frac{2 + \frac{a}{W}}{\left(1 - \frac{a}{W}\right)^{\frac{3}{2}}} \right] \left[0.866 + 4.64 \left(\frac{a}{W}\right) - 13.32 \left(\frac{a}{W}\right)^2 + 14.72 \left(\frac{a}{W}\right)^3 - 5.6 \left(\frac{a}{W}\right)^4 \right] \quad (3)$$

In Eq. 2 and 3:

P_Q: Critical load value (KN)

B: Sample Thickness

W: Sample Width

a: crack length

Fig. 13 shows the results of the fracture toughness test. By examining the charts obtained from the fracture toughness, the amount of fracture toughness for the 2 -2-layer sheet increased by about 160% compared to the Al base sheet and about 225% compared to the Mg base sheet. This is a sign of improved fracture toughness in two-layer samples. Applying cold work and increasing the strength and hardness can be one of the reasons for increasing the fracture toughness of the two-layer sample [35, 36]. The results of the fracture toughness test are briefly shown in Table 2.

3.5. Fractography

SEM imaging was performed on the tensile test sample to investigate the effect of the rolling process and the effect of different annealing temperatures on the fracture mode of the two-layer sample and compare it with the base sheet [40].

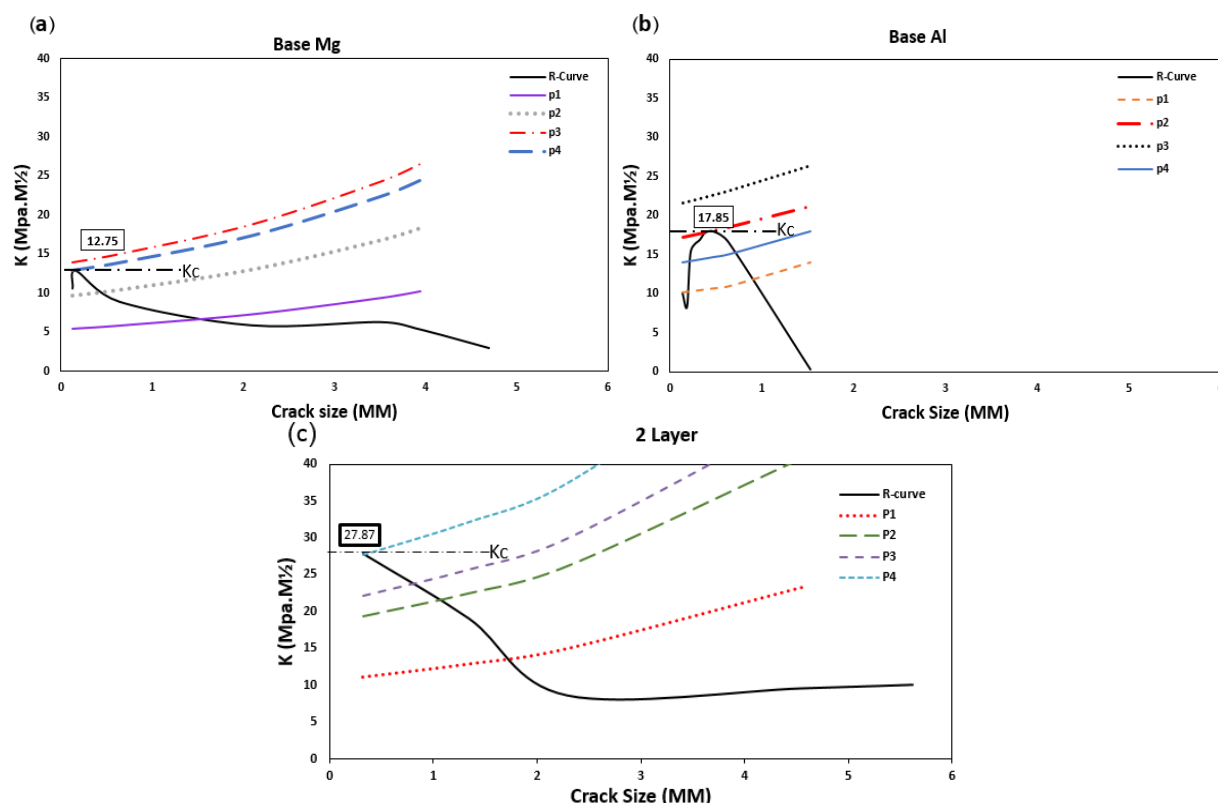


Fig. 13. R-curve graphs of the two-layer sample resulted from fracture toughness tests, a) Mg base sheet, b) Al base sheet, and c) two-layer sample

Table 2. Compression Fracture toughness and force result for the base and 2 Layer sample

Sample	Force (N)	Fracture toughness (MPa.M ^{1/2})
2 Layer	757	27.87
Al base	474	17.85
Mg base	355	12.75

According to Al (FCC) and Mg (HCP) crystal structure, ductile and brittle fractures can be expected for them, respectively. One of the effective parameters in determining the fracture mechanism in brittle metals is temperature. In metals with brittle behavior, the fracture mechanism will change from brittle to ductile with increasing temperature.

Among the reasons for the change in the failure mechanism, one can point out the decrease in the density of dislocations and, as a result, the need for less shear stress for the movement of slip plates. Among other reasons for brittle failure is secondary phase particles in the microstructure [41].

In Fig. 14, the SEM images related to the fracture surfaces of the two-layer sheet at ambient temperatures of 200°C, 300°C and 400°C can be seen.

In Fig. 15, the results for the base sheets are given. Fig. 14 a-b respectively show the fracture surfaces in the Al and Mg regions for the two-layer sheet at room temperature. Investigations show that the fracture mechanism is similar to the base sheets, and the change in the fracture type did not occur after the rolling process.

Only in the two-layer sample in the ductile fracture, the depth of the dimples decreased compared to the base sample, which indicates its lower formability.

In Fig. 14-d, it can be seen that at the annealing temperature of 200°C, the fracture mechanism in the two-layer sample on the Mg side is mixed, brittle, and ductile. At this temperature, grain growth occurs, and the intermetallic phases formed are not large enough in diameter to prevent dislocation movement. As a result, deformation and fracture occurred by slip and twinning mechanisms, leading to a combination of brittle and ductile fracture in the magnesium region. In the following, for the annealing temperatures of 300°C and 400°C, due to the formation of brittle secondary phases, the fracture mechanism has occurred in a brittle manner in the Mg region, and in the Al region, the fracture has still occurred with a ductile mechanism.

4. CONCLUSIONS

This research investigated the effect of the

rolling process on the strength of a 2-layer Al/Mg sample and the effect of mechanical and metallurgical properties and effective parameters on interlayer strength conditions. Below is a summary of the results obtained from this research.

- (1) For two-layer samples, EDS-Line analysis showed that the penetration depth would also increase with the increase of annealing temperature.
- (2) The uniaxial tensile test showed that the strength of the two-layer sample increased by about 120% compared to the Al base metal. On the other hand, it decreased by about 5% compared to the Mg base metal. Also, strength decreases with increasing temperature, increasing the ductility in the two-layer samples.
- (3) The most optimal annealing temperature for a two-layer sample in terms of strength and ductility is the 200°C annealing temperature, which increases the annealing temperature; in addition to reducing the formability, the strength will decrease.
- (4) The micro-hardness test results show the micro-hardness result for the two-layer sample increase compared to the base sheets.
- (5) The three-point bending results show that the bonding strength created in the two-layer samples is good and at the level of base metals.
- (6) The fracture toughness test performed on the base and two-layer sheet samples shows that the fracture toughness of the two-layer sheet has increased by 225% and 160%, respectively, compared to Mg and Al base sheets.
- (7) Examining the fracture results shows that at the annealing temperature of 200 degrees, the fracture mechanism in the Mg region of the two-layer sheet will change from brittle to brittle-ductile fracture. However, as the annealing temperature increases from 200°C to 400°C, brittle secondary phases will form, and the fracture in the Mg region will be brittle.

ACKNOWLEDGEMENTS

This work is based upon research funded by Iran National Science Foundation (INSF) under project No. 4013311.



Fig. 14. SEM images from the fracture surfaces, a) 2-layer Al section- room temperature, b) 2- layer Mg section- room temperature, c) 2- layer Al section-200°C, d) 2- layer Mg section-200°C, e) 2- layer Al section-300°C, f) 2- layer Mg section-300°C, g) 2- layer Al section-400°C, h) 2- layer Mg section-400°C

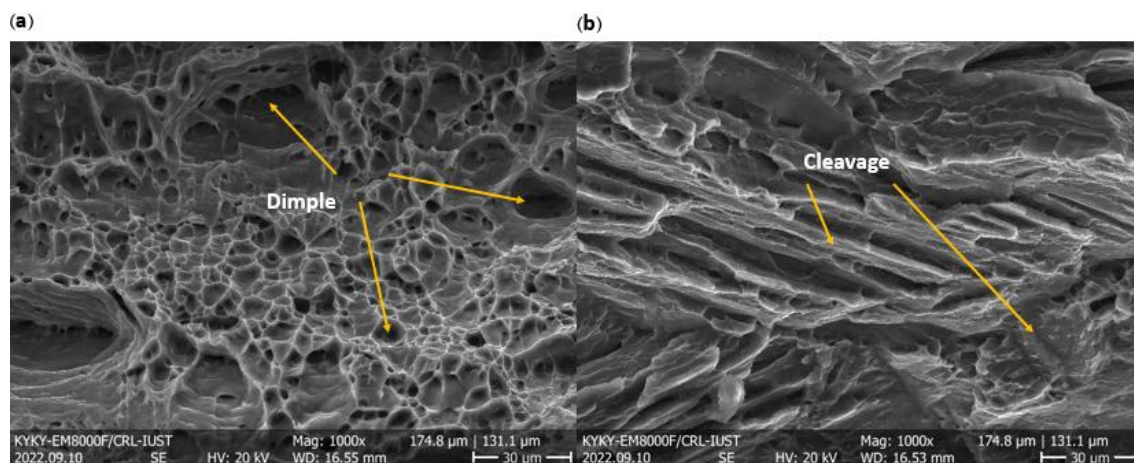


Fig. 15. SEM images from the fracture surfaces, a) Al Base sheet, b) Mg Base sheet

5. 4-REFERENCES

- [1]. Guang B, Song L, Atrens A. Corrosion Mechanisms of Magnesium Alloys **. 2000;11–33.
- [2]. Liu F, Liang W, Li X, Zhao X, Zhang Y, Wang H. Improvement of corrosion resistance of pure magnesium via vacuum pack treatment. *J Alloys Compd* 2008; 461:399–403.
<https://doi.org/10.1016/j.jallcom.2007.06.097>.
- [3]. Habila W, Azzeddine H, Mehdi B, Tirsatine K, Baudin T, Helbert AL, et al. Investigation of microstructure and texture evolution of a Mg/Al laminated composite elaborated by accumulative roll bonding. *Mater Charact* 2019; 147:242–52.
<https://doi.org/10.1016/j.matchar.2018.11.010>.
- [4]. Atifeh, S. M., Rouzbeh, A., Hashemi, R., & Sedighi M. Effect of annealing on formability and mechanical properties of AA1050/Mg-AZ31B bilayer sheets fabricated by explosive welding method. *Int J Adv Manuf Technol* 2022; 118:1–10.
<https://doi.org/https://doi.org/10.1007/s00170-021-07999-z>.
- [5]. Jinfeng Nie, Mingxing Liu, Fang Wang, Yonghao Zhao, Yusheng Li YC and Yuntian Z. Fabrication of Al / Mg / Al Composites via. *Materials (Basel)* 2016; 9:951. <https://doi.org/10.3390/ma9110951>.
- [6]. Cheepu M, Haribabu S, Ramachandriah T, Srinivas B, Venkateswarulu D, Karna S, et al. Fabrication and Analysis of Accumulative Roll Bonding Process between Magnesium and Aluminum Multilayers. *Appl Mech Mater* 2018; 877:183–9.
<https://doi.org/10.4028/www.scientific.net/amm.877.183>.
- [7]. Yu Y, Xue X, Lu Z, Li T, Ma C, Yan P, et al. Effect of Mg plate pretreatment on microstructure and mechanical properties of Al/Mg/Al laminated composites fabricated by hot roll bonding. *Int J Mod Phys B* 2020; 34:1–7.
<https://doi.org/10.1142/S0217979220400524>.
- [8]. Rouzbeh A, Sedighi M, Hashemi R. Comparison between Explosive Welding and Roll-Bonding Processes of AA1050/Mg AZ31B Bilayer Composite Sheets Considering Microstructure and Mechanical Properties. *J Mater Eng Perform* 2020; 29:6322–32. <https://doi.org/10.1007/s11665-020-05126-9>.
- [9]. Nie H, Liang W, Chen H, Zheng L, Chi C, Li X. Materials Science & Engineering A Effect of annealing on the microstructures and mechanical properties of Al/Mg/Al laminates. *Mater Sci Eng A* 2018; 732:6–13.
<https://doi.org/10.1016/j.msea.2018.06.065>.
- [10]. Macwan A, Jiang XQ, Li C, Chen DL. Effect of annealing on interface microstructures and tensile properties of rolled Al/Mg/Al tri-layer clad sheets. *Mater Sci Eng A* 2013; 587:344–51.
<https://doi.org/10.1016/j.msea.2013.09.002>.
- [11]. Jalali, A., R. Hashemi, M. Rajabi and PT. Finite element simulations and experimental verifications for forming limit curve determination of two-layer aluminum/brass sheets considering the

- incremental forming process. *Proc Inst Mech Eng Part L J Mater Des Appl* 2022; 236:361–73.
- [12]. Nie H, Chi C, Chen H, Li X, Liang W. Microstructure evolution of Al/Mg/Al laminates in deep drawing process. *J Mater Res Technol* 2019; 8:5325–35. <https://doi.org/10.1016/j.jmrt.2019.08.053>.
- [13]. Rahmatabadi D, Tayyebi M, Najafizadeh N, Hashemi R, Rajabi M. The influence of post-annealing and ultrasonic vibration on the formability of multilayered Al5052/MgAZ31B composite. *Mater Sci Technol (United Kingdom)* 2021; 37:78–85. <https://doi.org/10.1080/02670836.2020.1867784>.
- [14]. Gholami MD, Davoodi B, Hashemi R. Study of forming limit curves and mechanical properties of three-layered brass (CuZn10)/low carbon steel (St14)/brass (CuZn10) composite considering the effect of annealing temperature. *J Mater Res Technol* 2022; 18:4672–82. <https://doi.org/10.1016/j.jmrt.2022.04.118>.
- [15]. Rahmatabadi D, Pahlavani M, Gholami MD, Marzbanrad J, Hashemi R. Production of Al/Mg-Li composite by the accumulative roll bonding process. *J Mater Res Technol* 2020; 9:7880–6. <https://doi.org/10.1016/j.jmrt.2020.05.084>.
- [16]. Han J, Li S, Gao X, Huang Z, Wang T, Huang Q. Effect of annealing process on interface microstructure and mechanical property of the Cu/Al corrugated clad sheet. *J Mater Res Technol* 2023; 23:284–99. <https://doi.org/10.1016/j.jmrt.2022.12.188>.
- [17]. Nie H, Liang W, Chen H, Wang F, Li T, Chi C, et al. A coupled EBSD/TEM study on the interfacial structure of Al/Mg/Al laminates. *J Alloys Compd* 2019; 781:696–701. <https://doi.org/10.1016/j.jallcom.2018.11.366>.
- [18]. Luo C, Liang W, Chen Z, Zhang J. Effect of high temperature annealing and subsequent hot rolling on microstructural evolution at the bond-interface of Al/Mg/Al alloy laminated composites. *Mater Charact* 2013; 84:34–40. <https://doi.org/10.1016/j.matchar.2013.07.007>.
- [19]. Tayebi P, Fazli A, Asadi P, Soltanpour M. Formability analysis of dissimilar friction stir welded AA 6061 and AA 5083 blanks by SPIF process. *CIRP J Manuf Sci Technol* 2019; 25:50–68. <https://doi.org/10.1016/j.cirpj.2019.02.002>.
- [20]. ASTM E647–13. Standard Test Method for Measurement of Fatigue Crack Growth Rates. *Am Soc Test Mater* 2014:1–50. <https://doi.org/10.1520/E0647-15.2>.
- [21]. Jamaati R, Toroghinejad MR. Effect of friction, annealing conditions and hardness on the bond strength of Al/Al strips produced by cold roll bonding process. *Mater Des* 2010; 31:4508–13. <https://doi.org/10.1016/j.matdes.2010.04.022>.
- [22]. Reza Abbaschian, Robert E. Reed-Hill LA. *Physical Metallurgy Principles*. 4th ed. 2009.
- [23]. Payam Tayebi, Amir Reza Nasirin HA and RH. Experimental and Numerical Investigation of Forming Limit Diagrams during Single Point Incremental Forming for Al/Cu. *Metals (Basel)* 2024; 14:214. <https://doi.org/https://doi.org/10.3390/met14020214>.
- [24]. Wang P, Huang H, Liu J, Liu Q, Chen Z. Microstructure and mechanical properties of Ti6Al4V/AA6061/AZ31 laminated metal composites (LMCs) fabricated by hot roll bonding. *J Alloys Compd* 2021; 861. <https://doi.org/10.1016/j.jallcom.2020.157943>.
- [25]. Zhang N, Wang W, Cao X, Wu J. The effect of annealing on the interface microstructure and mechanical characteristics of AZ31B/AA6061 composite plates fabricated by explosive welding. *J Mater* 2014; 65:1100–9. <https://doi.org/10.1016/j.matdes.2014.08.025>.
- [26]. Werb DAN. Experimental investigation of the Mg/Al phase diagram from 47 to 63 at.% Al. *J Alloy Compd* 1997; 247:57–65.
- [27]. J. D. Hanawalt, H. W. Rinn and LKF. *Chemical Analysis by X-Ray Diffraction*. *Ind Eng Chem Anal* 1938:457–512. <https://doi.org/https://doi.org/10.1021/ac50125a001>.
- [28]. Jafarian M, Rizi MS, Javadinejad R, Ghaheri A, Taghi M. Effect of thermal tempering on microstructure and mechanical properties of Mg-AZ31/Al-6061 diffusion bonding. *Mater Sci Eng A* 2016; 666:372–9. <https://doi.org/10.1016/j.msea.2016.04.011>.
- [29]. Meifeng H, Lei L, Yating W, Cheng Z, Wenbin H. Influence of microstructure on

- corrosion properties of multilayer Mg–Al intermetallic compound coating. *Corros Sci* 2011; 53:1312–21. <https://doi.org/10.1016/j.corsci.2010.12.029>.
- [30]. Bae JH, Prasada Rao AK, Kim KH, Kim NJ. Cladding of Mg alloy with Al by twin-roll casting. *Scr Mater* 2011; 64:836–9. <https://doi.org/10.1016/j.scriptamat.2011.01.013>.
- [31]. Liu XB, Chen RS, Han EH. Preliminary investigations on the Mg–Al–Zn/Al laminated composite fabricated by equal channel angular extrusion. *J Mater Process Technol* 2009; 209:4675–81. <https://doi.org/10.1016/j.jmatprotec.2008.11.034>.
- [32]. Zhao LM, Zhang ZD. Effect of Zn alloy interlayer on interface microstructure and strength of diffusion-bonded Mg–Al joints. *Scr Mater* 2008; 58:283–6. <https://doi.org/10.1016/j.scriptamat.2007.10.006>.
- [33]. Gu L, Meng A, Chen X, Zhao Y. Simultaneously enhancing strength and ductility of HCP titanium via multi-modal grain induced extra $\langle c+a \rangle$ dislocation hardening. *Acta Mater* 2023; 252:118949. <https://doi.org/10.1016/j.actamat.2023.118949>.
- [34]. Tayebi P, Hashemi R. Study of single point incremental forming limits of Al 1050/Mg-AZ31B two-layer sheets fabricated by roll bonding technique: Finite element simulation and experiment. *J Mater Res Technol* 2024; 29:149–69. <https://doi.org/10.1016/j.jmrt.2024.01.085>.
- [35]. Bagheri A, Shabani A, Toroghinejad MR, Taherizadeh A. Post-rolling annealing of a multilayered Brass/IFS/Brass composite: An evaluation of anisotropy, formability, and mechanical properties. *J Mater Res Technol* 2022; 19:732–46. <https://doi.org/10.1016/J.JMRT.2022.05.037>.
- [36]. Peng XK, Wuhner R, Heness G, Yeung WY. On the interface development and fracture behaviour of roll bonded copper/aluminium metal laminates. *J Mater Sci* 1999; 34:2029–38. <https://doi.org/10.1023/A:1004543306110>.
- [37]. Zhang X, Yu Y, Liu B, Ren J. Mechanical properties and tensile fracture mechanism investigation of Al/Cu/Ti/Cu/Al laminated composites fabricated by rolling. *J Alloys Compd* 2019; 805:338–45. <https://doi.org/10.1016/j.jallcom.2019.07.064>.
- [38]. Tayebi P, Hashemi R. Numerical and experimental study of three-layered Al 1050/Mg AZ31B/Al 1050 sheets formability considering strain and stress conditions through single point incremental forming. *Mater Today Commun* 2024; 41:110884. <https://doi.org/10.1016/j.mtcomm.2024.110884>.
- [39]. Mourad AHI, Alghafri MJ, Abu Zeid OA, Maiti SK. Experimental investigation on ductile stable crack growth emanating from wire-cut notch in AISI 4340 steel. *Nucl Eng Des* 2005; 235:637–47. <https://doi.org/10.1016/j.nucengdes.2004.10.005>.
- [40]. Darban H, Mohammadi B, Djavanroodi F. Effect of equal channel angular pressing on fracture toughness of Al-7075. *Eng Fail Anal* 2016; 65:1–10. <https://doi.org/10.1016/j.engfailanal.2016.03.010>.
- [41]. Dieter GE. *Mechanical Metallurgy*. McGraw-Hill; 1961.